Electromagnetic scattering in two-dimensional dissipative systems without localization

H. Spieker and G. Nimtz
II. Physikalisches Institut, Universität zu Köln, Zülpicher Strasse 77, D-50937 Köln, Germany
(Received 1 February 1996)

Two-dimensional microwave propagation is experimentally studied in strongly scattering and absorbing random media. The results are compared with adapted theories of Genack, Ferrari, and Kaveh, as well as with classical diffusion theory. The diffusion constants and propagation velocities are determined. Most metallic or semiconductor system's localization effects, if they exist, are so weak that a classical description of the system is appropriate within measuring resolution. [S1063-651X(96)05310-X]

PACS number(s): 03.40.Kf, 41.20.Jb, 72.15.Ru

I. INTRODUCTION

Propagation of electromagnetic waves in random media has achieved a large amount of interest in the last decade (for a review see [1,2]). The investigation of weak and strong localization with light and microwaves as well as the diffusing velocity, i.e., the velocity connecting the diffusion constant D and the mean-free-path l, are of major importance. Understanding of these characteristics in the case of electromagnetic waves will support analog work on electrons, where many more side effects (Coulomb interaction, electron-electron-interaction, etc.) have to be considered, which can cover the pure localization effects (review in [3]).

II. EXPERIMENTAL SETUP

The experiments were carried out with microwaves in the frequency ranges of [20–24 GHz] and [36–40 GHz]. The microwaves were confined in the space between two quadratic aluminum plates of 60 cm-length of side (see Fig. 1). The plates were about 1.6 mm apart. So even for the hightest frequency of 40 GHz the vacuum wavelength is more than a factor of 4 larger than the plates' distance of 1.6 mm. This implies the electric field of the microwaves to be perpendicular to the plates and the microwaves will propagate parallel to the plates, i.e., the experimental setup presents a two-dimensional guide.

Metallic disks (the scatterers) are placed randomly between the plates. They have a height of 1.6 mm and a diameter of 19.3 mm, about the same order of magnitude as the wavelengths. Since the electric contacts between the disks and the plates are not ideal and the conductivity of the disks and the aluminum plates is finite, the guiding system will have dissipative losses.

The border of (the space between) the plates is alternatively left open or closed with aluminum foil to get a measure for the influence of the border. In the open case there are additional losses in consequence of radiation into the environment, whereas in the closed case the microwaves are reflected back. The microwaves are coupled into the two-dimensional system and detected via antennae probes. The latter reach between the plates through holes in the upper plate (see Fig. 1).

The holes are discontinuities and also scatter the microwaves, but since they are only about a tenth of the disks and about a third of the smallest wavelength, their influence is neglected further on. The two antennae probes are connected to the ports of a so-called test set, which allows, in combination with a network analyzer, a microwave source and a standard calibration technique (TRM calibration, cf. [4]), to measure the transmitted microwaves vectorially, i.e., in amplitude and phase (dynamic range >90 dB, i.e., nine decades in energy). In particular this allows the direct measurement of the group velocity and the autocorrelation function of the electric field, as well as to Fourier transform into time domain. The investigated distances between the antennae are 4, 6, 14, 24, and 34 cm. The antennae are placed as near to the center of the plates as possible in order to maximize the distance to the edge and to minimize its influence on the measurement.

The scatterers are placed randomly at surface filling factors of 10%, 20%, 25%, 30%, 35%, and 40%. For each of these filling factors and both frequency ranges there are prepared five random configurations of scatterers without aluminum foil at the edge and one random configuration with aluminum foil at the edge. And for each of these configurations the transmission is measured for the five antennae distances.

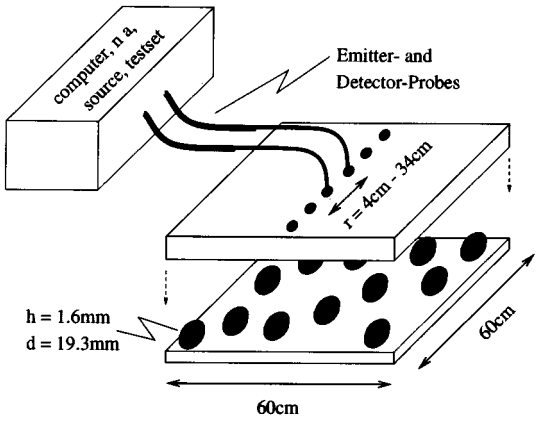

FIG. 1. The experimental setup consists of two quadratic aluminum plates of 60 cm length of side. On the lower one the metallic scatterers are placed randomly. The upper one has holes for the antennae, which are built of coaxial wires, with slightly longer inner conductors. The main instruments are shown schematically in the box: computer, network analyzer, microwave source, (so-called) test set.

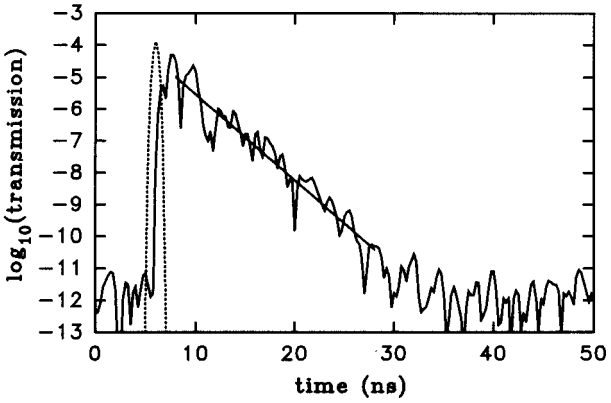

FIG. 2. Typical Fourier transformed data for fitting the energy-decay rate of a measurement in the frequency range [20–24 GHz] with 20% filling factor and 14 cm antenna distance. The dotted line shows the assumed input pulse normalized to the total transmitted intensity. The offset from zero time is due to run time in the antenna wires.

Each frequency range consists of 801 frequency points, 5 MHz apart. So for the Fourier transformed data we get a time range of 200 ns with a resolution of 0.25 ns.

III. RESULTS

In the following subsections we present the experimental data for the absorption time τ_{abs}, the diffusion constant in the classical diffusion picture D_{cl}, the group velocity v_g, the velocity of the center of gravity v_s, the center of gravity time t_S, and the autocorrelation function G^E. These values are averages over each frequency range, and in the case of open edge over five configurations.

A. Energy-decay rate

The energy-decay rate (reciprocal absorption time) $1/\tau_{\text{abs}}$ for each configuration is determined via Fourier transform of the transmitted electric field, into the time domain and fitting the decaying part of the intensity to an exponential function of the form $I_0 \exp(-t/\tau_{\text{abs}})$. An example is shown in Fig. 2. This τ_{abs} is an implicit average over the frequency range of the Fourier transform. The damping of each frequency component depends strongly on its intensity distribution inside of each configuration, since the losses are caused mainly by currents in the metal plates and by radiation at the edges.

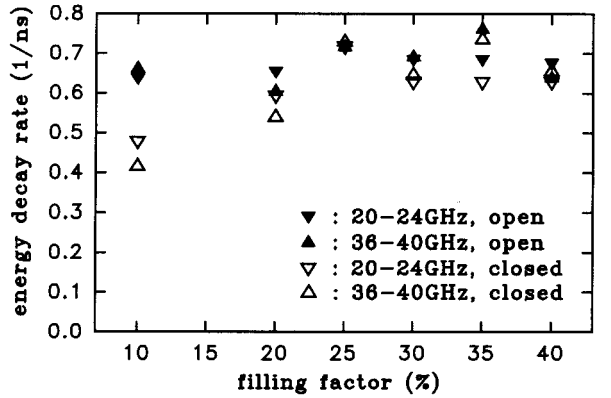

FIG. 3. The energy-decay rate (reciprocal absorption time) vs the filling factor for both frequency ranges with open and (metallic) closed edge. The values are averages over each frequency range, over antennae distances, and in the case of open edge over five configurations. The average errors were determined to 0.011/ns for the open-edge data and 0.025/ns for the closed-edge data.

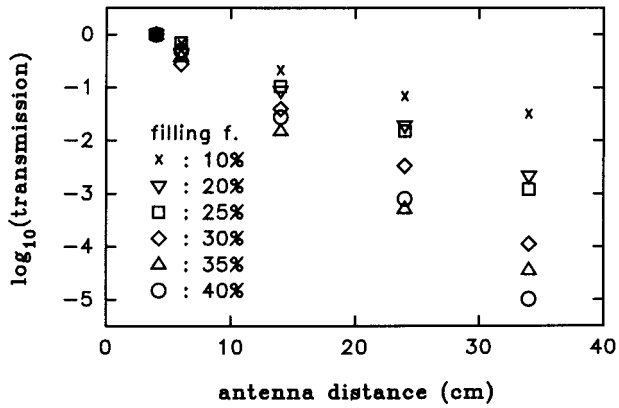

FIG. 4. Mean transmitted intensity $[\propto N(x)]$ as function of antenna distance for the frequency range [20–24 GHz] in the open-edge case (averaged over five configurations and normalized to the 4-cm values). The frequency range [36–40 GHz] has a similar behavior, not shown here. The average errors are about the symbol size.

In Fig. 3 the energy-decay rate is shown as a function of filling factor of scattering centers for the two frequency ranges with open and with metallic reflecting edge. The values are averages over the five different antennae distances. For the open edge the values seem to be nearly independent of the filling factor. But for the metallic reflecting edge the losses get stronger with increasing filling factor and come close to the open edge case for 25% filling factor. So the independency for the open-edge case is the consequence of two effects, the losses at the scatterers and the losses due to radiation at the edge. The first one increases with the filling factor and the latter one gets weaker with increasing filling factor, since less energy reaches the edge due to increased

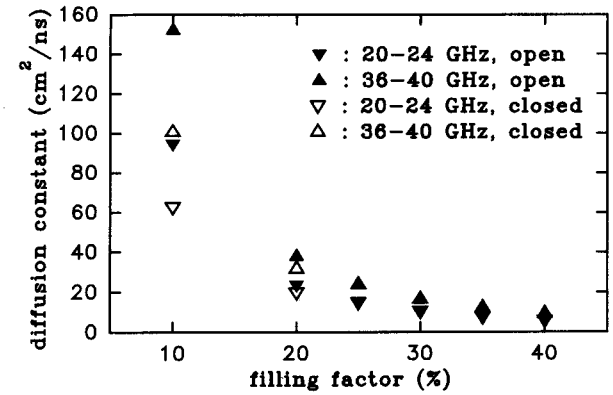

FIG. 5. Diffusion constant vs filling factor for both frequency ranges.

TABLE I. Group velocity as a function of the scatterer filling factor in units of the vacuum velocity of light.

Filling factor (%)	10	20	25	30	35	40
20–24 GHz (units of c_0)	0.43±0.04	0.28±0.02	0.28±0.02	0.24±0.01	0.23±0.01	0.23±0.01
36–40 GHz (units of c_0)	0.40±0.04	0.30±0.02	0.27±0.02	0.26±0.02	0.26±0.02	0.20±0.01

scattering and absorption inside the medium. These two effects compensate each other and lead to nearly no dependence of the absorption time on the filling factor for the open-edge case (in the used experimental setup). Consequently the losses due to the scatterers itself are best represented by the energy-decay rate for the closed edge case. This rate will be used further on for calculations.

B. Diffusion constant in the particle picture

To determine the diffusion constant in the particle picture we make the following assumptions: (a) the microwaves diffuse like particles (random walk, no interference), (b) the edge is neglected (infinite medium), and (c) the absorption is uniform across the medium, with the absorption time found in the closed-edge case. From the diffusion equation $dN/dt=-N/\tau_{\rm abs}+D_{\rm cl}\Delta N$, with N the number density of particles (here the energy density of microwaves), t the time, $D_{\rm cl}$ the (classical) diffusion constant, and $\tau_{\rm abs}$ the absorption time, one obtains the following solution for N in two dimensions in the steady state: $N(x)=c_1I_0(x)+c_2K_0(x)$. $x\equiv r/(D_{\rm cl}\tau_{\rm abs})^{1/2}$ is the normalized distance from the source (antenna), where r is the real distance from the source, c_1 and c_2 are integration constants, and $I_0(x)$ and $K_0(x)$ are modified Bessel functions of zeroth order and first or second kind, respectively. Since $\lim_{x\to\infty}I_0(x)=\infty$ the integration constant c_1 has to be zero for an infinite medium without reflecting edges. So for fitting to experimental data (see Fig. 4) and assuming an infinite sample there are only two parameters left: the integration constant c_2 and the product of $\tau_{\rm abs}D_{\rm cl}$. From the latter one and with the knowledge of $\tau_{\rm abs}$ from the Fourier transformed data we obtain $D_{\rm cl}$. The values are shown in Fig. 5 as a function of the filling factor. They decrease from about 100 $\rm cm^2/ns$ for 10% filling factor to about 8 $\rm cm^2/ns$ for 40% for both frequency ranges. The 10% values are too large due to the influence of the edge (increased losses).

With this diffusion constant the diffusion velocity is $v_D=2D_{\rm cl}/l$ with mean free path l in two dimensions. Until 1991 it had been widely expected that the phase velocity for v_D would be found, but since the work of van Albada *et al.* [5] the energy transport velocity v_E is considered, which should account for time delays due to resonances in the scattering process. As there is no way to measure the mean free path with our setup directly, we have carried out a computer simulation, i.e., we put a particle randomly into the sample and let it move forward until it hits a scatterer. Particle diameters, half the average wavelengths (this is the cutoff wavelength in rectangular wave guides) of the investigated frequency ranges are chosen (1.36 and 0.79 cm). The results are shown in Fig. 6. With this data the diffusion velocities are determined. They range from about $1.3c_0$ to $0.4c_0$ (c_0 is the vacuum velocity of light), for the two frequency ranges and six filling factors. They decrease with increasing filling factor and are higher for the upper-frequency range. For 10% filling factor the velocity is higher than c_0 due to the influence of the edge (compare the values of the diffusion constant).

C. Group velocity

Since our setup is capable of measuring vectorially, we directly find the center-of-gravity time $t_S\equiv d\varphi/d\omega$, with φ the phase shift (modulo 2π) during transmission and $\omega\equiv 2\pi\nu$ the angular frequency. Plotting the center-of-gravity time against antennae distance will directly show the group velocity v_g as the reverse slope. For diffusing particles one would normally expect the center-of-gravity time to be proportional to the square of the antennae distance, but as absorption takes place the longer paths are stronger attenuated than the shorter ones and we get a linear dependence for long enough times: $t=0.5\ \tau_{\rm abs}\ (0.5+r/l_{\rm abs})$ for $r\gg l_{\rm abs}$ ($l_{\rm abs}\equiv\sqrt{D_{\rm cl}\tau_{\rm abs}}$; more details are given in Sec. III E and [7]). Group velocities determined by this procedure are shown in Table I as a function of the filling factor.

D. Velocity of the center of gravity

The velocity of the center of gravity v_s is determined from the data in the time domain. The times are weighted with the transmitted intensity at that time and then averaged. For the velocity of the center of gravity v_s one gets nearly the same values as for the group velocity. Table II shows v_s as a function of filling factor.

E. Center of gravity time

As mentioned above the center-of-gravity time is linearly dependent on the antennae distance for long enough times.

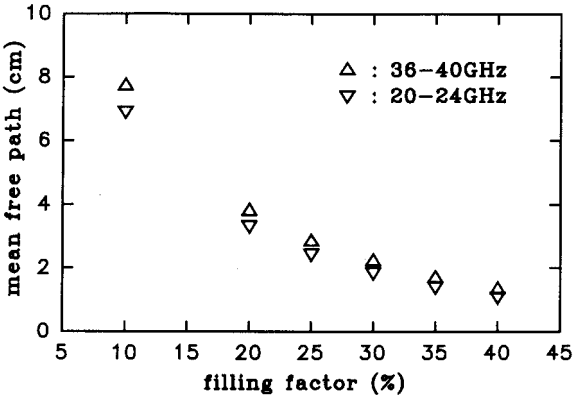

FIG. 6. Simulated values for the mean free path as a function of the filling factor. The extension of the diffusing particle is taken to be the half wavelength of the middle frequency of each frequency range.

TABLE II. Velocity of the center of gravity as a function of the scatterer filling factor in units of the vacuum velocity of light.

Filling factor (%)	10	20	25	30	35	40
20–24 GHz (units of c_0)	0.42±0.05	0.30±0.02	0.25±0.02	0.23±0.01	0.20±0.01	0.14±0.01
36–40 GHz (units of c_0)	0.46±0.06	0.32±0.03	0.30±0.02	0.24±0.02	0.20±0.01	0.19±0.01

For shorter times the behavior is different. To calculate the center-of-gravity time one has to take the average of the times for the different paths on which a particle can diffuse the distance between the two antennae weighted with its probability.

$$t_S(r)=\frac{\int_0^\infty t p(r,t)dt}{\int_0^\infty p(r,t)dt},$$

with $p(r,t)=(4\pi Dt)^{-d/2}\exp[-r^2/(4Dt)]\exp(-t/\tau_{\rm abs})$ the probability density in d dimensions to diffuse in time t on a path between two points (antennae) which are a distance r apart. Substituting $x\equiv r/(D\tau_{\rm abs})$ and further transformations lead to

$$t_S(x)=0.5x\tau_{\rm abs}\mathcal{I}_{1-d/2}(x)/\mathcal{I}_{-d/2}(x),$$

with

$$\mathcal{I}_n(x)\equiv\int_1^\infty[(z-\sqrt{z^2-1})^{n+1}+(z+\sqrt{z^2-1})^{n+1}]\sqrt{z^2-1}^{-1}\exp(-xz)dz.$$

Simple solutions are available in one and three dimensions: $t_{S,d=1}(x)=\tau_{\rm abs}(1+x)/2$ and $t_{S,d=3}(x)=\tau_{\rm abs}x/2$. For two dimensions we have simpler formulas only in the extremal cases $x\to 0$ and $x\to\infty$: $t_{S,d=2}(x\to 0)=\tau_{\rm abs}/(2\ln 2/x\gamma)$ and $t_{S,d=2}(x\to\infty)=\tau_{\rm abs}(0.5+x)/2$ with $\gamma\equiv e^C$, C the Euler constant (0.577 216...). For nonextremal values of x the integrals have to be numerically solved in two dimensions.

The results are displayed together with the experimental data in Fig. 7. For small distances the experiment yields too high values for the center-of-gravity time, but for larger distances the data fit better to the theoretical curve. The cause

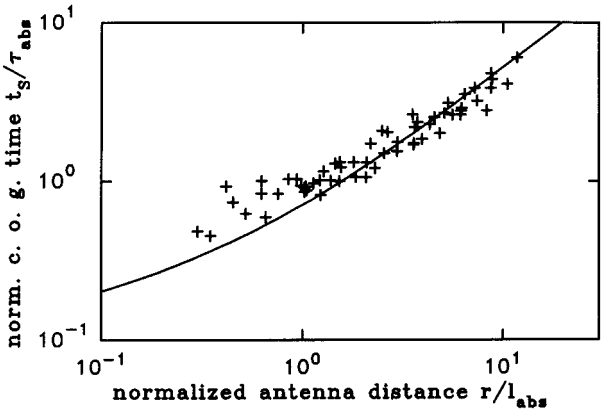

FIG. 7. Double logarithmic plot of normalized center-of-gravity time for diffusion vs normalized antennae distance. The continuous line is the theoretical curve for two dimensions, the crosses are the experimental data, with $\tau_{\rm abs}$ and D from Secs. III A and III B.

for the behavior at low values of x, i.e., $r\ll l_{\rm abs}$, could be the failing of the diffusion equation for distances in the order of the mean-free-path (no statistical independent scattering events). The statistical character of particle motion gets lost and the transfer from one antenna to the other is dominated by some kind of cavity (resonator) buildup by the surrounding scatterers. So the center-of-gravity time stays above some positive value, even for closest antennae and does not approach zero as expected for ideal diffusive propagation.

F. Autocorrelation function and model of Genack

Until now we have neglected interference effects, i.e., the wave character in the propagation of microwaves. The implementation of it will be done in the following. Using a path summation ansatz, as shown by Genack in [6], we calculate the autocorrelation function of the electric field and compare it with measured data. Usually the intensity autocorrelation function is calculated, since most published experiments were not able to measure vectorially, which is necessary to determine the electric field autocorrelation function. But since our setup measures vectorially we can directly compare with the electric field autocorrelation function.

The ansatz is to write the electric field received by one antenna in the steady state as the sum of the contributions of the differents paths leading to this antenna,

$$E(\nu)=\sum_\alpha p(\alpha)\exp[i\Phi(\alpha,\nu)]$$

with $p(\alpha)$ the real probability amplitude on path α, so that the configurational average of $\Sigma_{\alpha:s<s_\alpha<s+ds}p^2(\alpha)$ equates the probability for path lengths in the range of s and $s+ds$: $P(s)ds$. And $P(s)$ again is taken from the diffusion picture, neglecting the wave character. $\Phi(\alpha,\nu)$, the phase, is divided into a part that depends on ν and a part that is caused from scattering and should not depend on ν: $\Phi(\alpha,\nu)=2\pi s_\alpha\nu/c+\Phi'(\alpha)$. With this assumption the autocorrelation function, defined as $G^E(\Delta\nu)\equiv{\rm Re}\langle E(\nu)E^*(\nu+\Delta\nu)\rangle$ is calculated to

$$G^E(\Delta\nu)\propto\int_0^\infty e^{-1/z}z^{-d/2}e^{-Az}\cos(2\pi Bz)dz$$

with dimensionality d, $A\equiv r^2/(4D\tau_{\rm abs})$, and $B=B(\Delta\nu)\equiv\Delta\nu/(4D)$. So the autocorrelation function is only dependent on the two dimensionless parameters A and B, and one can calculate the half-width of the autocorrelation function for comparison with experiment. In the range of $0.01<A<100$ one gets approximately

$$D=(28\pm 3)r^2\delta\nu^{(2.27\pm 0.05)}\tau_{\rm abs}^{(1.27\pm 0.05)}$$

with the half-width of the autocorrelation function $\delta\nu$. So for samples with the same diffusion constant and same absorption time (same filling factor) the half-width should approximately be inversely proportional to the antennae distance. But though our experiments have antennae distances ranging from 4 to 34 cm, the half-width only changes less than a factor of 2. If one tries to calculate the diffusion constant with the above equation it looks even worse. For example, in the case of a filling factor of 30% and the frequency range of 20–24 GHz the values for D reach from 0.13 cm^2/ns for $r=4$ cm to 5.2 cm^2/ns for $r=34$ cm. This discrepancy indicates that the ansatz of Genack cannot be applied to our experiment or the used assumptions are too restrictive. From the pure particle diffusion picture we get $D_{\mathrm{cl}}=10$ cm^2/ns (see Sec. III B). This is also in contrast to the values of the autocorrelation function by at least a factor of 2. The following points may be worth theoretical reconsideration: (a) $P(s)$ is taken from the particle diffusion picture, (b) the diffusion velocity is independent of frequency, and (c) $\Phi'(\alpha)$ does not depend on frequency.

G. Model of Ferrari

A further model that tries to incorporate the wave character of the electromagnetic radiation into its propagation description comes from Ferrari [8]. He finds the frequency distance $\Delta\nu$ between intensity maxima for a three-dimensional model to be equal to half of the reciprocal transmission time T through the sample: $\Delta\nu=0.5/T$. Further he calculates T from a one-dimensional diffusion equation under consideration of absorption and gets $\Delta\nu=0.5\,D\,(l_{\mathrm{abs}}^{-2}+\pi^2\,L^{-2})$, with L the system size and l_{abs} the absorption length $(=\sqrt{D\tau_{\mathrm{abs}}})$. To get a measure for the frequency distance between intensity maxima one can take the full width at half maximum (FWHM) of the transmitted intensity (as a function of frequency). This value results from the autocorrelation function of the electric field (with frequency). Inserting the experimental values for the FWHM of the autocorrelation function and the energy-decay-rate results in diffusion constants that strongly depend on antennae distance ([0.013 cm^2/ns; 0.019 cm^2/ns] for $r=4$ cm and [0.27 cm^2/ns; 0.79 cm^2/ns] for $r=34$ cm, depending on filling factor also) and which have values that are below some reasonable minimum values (assuming the mean-free-path $l>1$ cm and diffusion velocity $c>0.1c_0$). The values are shown in Fig. 8 as the area labeled ''Ferrari.''

H. Model of Kaveh

Another model that incorporates the wave character into the diffusion picture was published by Kaveh [9]. He calculates the probability of a diffusing wave packet to hit his own path again (the width of the wave packet is assumed to be the central wavelength λ). So he gets $D=0.5\,cl\,[1-0.5\lambda l^{-1}\pi^{-2}\ln(L/l)]$. In this case L is the minimum of system size and $\sqrt{D\tau_\varphi}$ with τ_φ the time in which the phase information of the wave gets lost (phase coherence time, which is for microwave experiments usually so large that it can be neglected). This formula is analogous to the ones found in the electronic case (see, e.g., [10,11]). To incorporate the influence of losses into this formula (which are present in our experiments) one has to consider that they reduce the probability

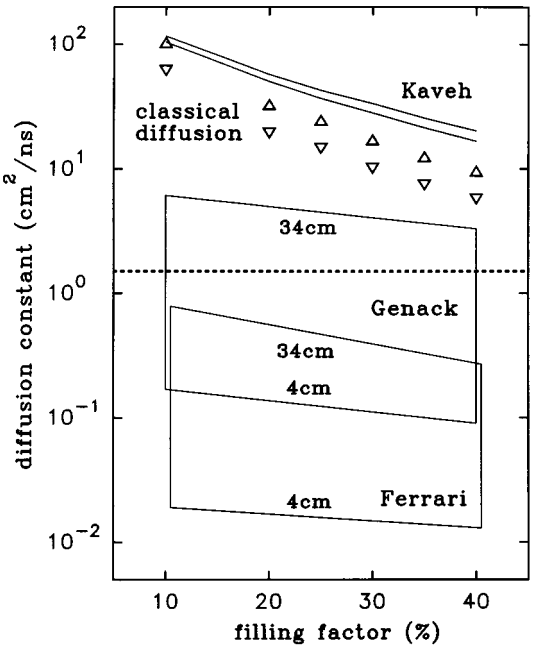

FIG. 8. Logarithmic plot of diffusion constants calculated from the different models against filling factor for both frequency ranges. The areas represent the ranges of the values in the models of Genack and Ferrari, where the values increase from the lower boundary to the upper boundary with increasing antennae distance. The triangles show the values of the classical diffusion model (▽, [20–24 GHz]; △, [36–40 GHz]). The lines show the values corresponding to the Kaveh model (lower line, [20–24 GHz]; upper line, [36–40 GHz]). The dashed line is a plausibility limit ($l>1$ cm, $c>0.1c_0$).

for long paths and so lessen the interference parts. Apparently, the losses have, in this model, the same influence on the diffusion constant as the phase coherence time. So one could redefine L to be the minimum of the system size and the absorption length $l_{\mathrm{abs}}\equiv\sqrt{D\tau_{\mathrm{abs}}}$ (neglecting the phase coherence time). Since the system size is 60 cm and l_{abs} ranges from about 3 cm to about 12 cm (experimental values from the classical diffusion model) one can substitute L by l_{abs}. Further we take λ to be the vacuum wavelength of the middles of the frequency ranges and the diffusion velocity to be the vacuum velocity of light, as one would have taken at the time of Kaveh's paper. A short calculation shows that the correction term (due to interferences) to the classical diffusion constant is less than 10% and can (under consideration of the width of the frequency ranges and the roughness of the mean-free-path simulation) be neglected in the following. What is left is the classical diffusion constant with a diffusion velocity of c_0. Inserting the simulated mean-free-path values leads to diffusion constants that are about a factor of 2–2.5 larger than the experimental values of our first classical model (which did not require any special values for the diffusion velocity). These diffusion constants are also shown in Fig. 8 as the lines. They do not depend on antennae distance and are in a reasonable range (in contrast to the former two nonclassical models of Genack and Ferrari). Furthermore, we achieve better agreement to the pure classical model if we substitute the vacuum velocity (which is used as the value for the diffusion velocity in the Kaveh model) by a

value of about $0.4c_0$, which is an energy transport velocity between the scatterers as proposed by van Albada *et al.* [5].

IV. SUMMARY

We have used a classical diffusion model as well as adapted models of Genack, Ferrari, and Kaveh to describe our experimental results for the propagation of microwaves between absorbing scattering centers in two dimensions. The diameters of the scattering centers were of the same order of magnitude as the wavelengths of the microwaves. The models of Genack and Ferrari could not describe our experimental values properly, but the classical model and the model of Kaveh has lead to reasonable results. The classical model and the model of Kaveh could be brought to good mutual agreement by inserting a value of about $0.4c_0$ into the diffusion velocity in the Kaveh model instead of c_0, supporting ideas of van Albada *et al.* of an energy transport velocity between the scatterers as the effective diffusion velocity.

ACKNOWLEDGMENTS

We wish to thank V. Gasparian and A. Enders for helpful discussions.

[1] *Scattering and Localization of Classical Waves in Random Media*, edited by Ping Sheng (World Scientific, Singapore, 1990).
[2] *Photonic Band Gaps and Localization*, edited by C. M. Soukoulis (Plenum, New York, 1993).
[3] P. A. Lee and T. V. Ramakrishnan, Rev. Mod. Phys. **57**, 287 (1985).
[4] H. J. Eul and B. Schiek, IEEE Trans. Microwave Theory Tech. **39**, 724 (1991).
[5] M. P. van Albada, B. A. van Tiggelen, A. Lagendijk, and A. Tip, Phys. Rev. Lett. **66**, 3132 (1991).
[6] A. Z. Genack, in *Scattering and Localization of Classical Waves in Random Media* (Ref. [1]).
[7] H. Spieker, Ph.D. thesis, Universität zu Köln, 1995 (unpublished).
[8] L. A. Ferrari, Nuovo Cimento **14 D**, 843 (1992).
[9] M. Kaveh, Philos. Mag. B **56**, 693 (1987).
[10] L. P. Gor'kov, A. I. Larkin, and D. E. Khmel'nitskiĭ, Pis'ma Zh. Eksp. Teor. Fiz. **30**, 248 (1979) [JETP Lett. **30**, 228 (1979)].
[11] M. Kaveh and N. F. Mott, J. Phys. C **14**, L177 (1981).